Desalination 452 (2019) 132–140

Contents lists available at ScienceDirect

Desalination

journal homepage: www.elsevier.com/locate/desal

Performance evaluation of a thermoresponsive polyelectrolyte draw solution in a pilot scale forward osmosis seawater desalination system

Mansour Ahmed*, Rajesha Kumar, B. Garudachari, Jibu P. Thomas

Water Research Center, Kuwait Institute for Scientific Research, P.O. Box 24885, 13109 Safat, Kuwait

GRAPHICAL ABSTRACT

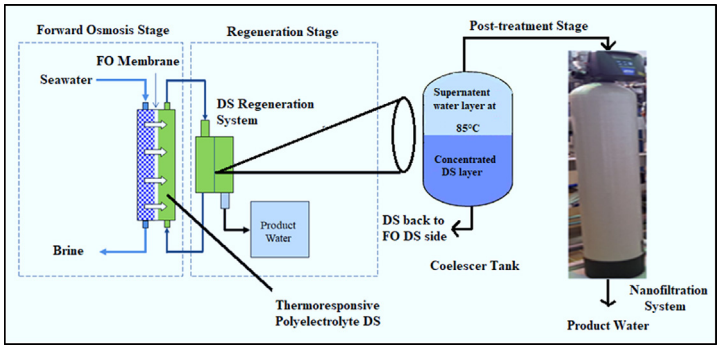

ARTICLE INFO

Keywords:
Forward osmosis
Thermo-responsive polyelectrolyte
Hollow fiber membrane
Bore diameter
Water recovery

ABSTRACT

The current study assesses the technical feasibility of using a thermoresponsive polyelectrolyte draw solution (DS) in a Forward Osmosis (FO) desalination pilot scale system of 10 m^3/day capacity. The FO system utilized a commercial spiral wound hollow fiber FO membrane and ethylene oxide-propylene oxide copolymer as DS. This study evaluated the effect of DS flow rate and feed solution flow rates on the net water recovery and product water flow rates of the system. The osmotic pressure distribution of polyelectrolyte DS at different sections of the HF module was greatly influenced by DS flow rate. The study revealed that the DS had great potential to generate the high osmotic pressure ($\Delta\pi$) difference in the various compartments of the HF module. The reliability of the FO pilot plant was proved over a long run without any severe FO membrane fouling with total dissolved solids of product water at 143 ppm and water recovery of 30%. The selected DS showed its potentiality towards the installation of commercial-scale FO desalination plant by witnessing its low viscosity and easy phase separation at a moderately lower temperature of 85 °C in the coalesce DS regeneration system.

1. Introduction

To tackle the scarcity of fresh water across the globe reverse osmosis (RO) desalination technologies are currently replacing the thermal-based technologies especially like multistage flash desalination plants. The proportion of desalination capacity supplied by RO is increasing due to its better economics when compared with multistage flash (MSF) process. However, the future of any desalination technology soon relies on its easy access for integration with renewable energy [1]. The high-pressure requirement by the RO membrane process may grab more site area for the installation of solar panels and large-scale integration with solar energy. To address the issues of the low energy desalination

* Corresponding author.
E-mail address: mahmed@kisr.edu.kw (M. Ahmed).

https://doi.org/10.1016/j.desal.2018.11.013
Received 29 August 2018; Received in revised form 9 November 2018; Accepted 17 November 2018
Available online 21 November 2018
0011-9164/

technology like forward osmosis is gaining much attention during the past one decade. The research studies show that the forward osmosis (FO) membrane process has a high potential for seawater desalination applications and can be one of the sustainable solutions for seawater desalination in near future [2,3]. FO has the potential to lower energy consumption in the seawater desalination process compared to RO process due to the absence of high hydraulic pressure pumps [4]. FO is driven by the osmotic pressure difference between the feed and the draw solutions and eliminates the need for high hydraulic pressure. In the FO process, water spontaneously permeates through a semipermeable membrane from the feed solution at a lower osmotic pressure to the draw solution at a higher osmotic pressure. A regeneration process extracts water from the diluted draw solution and re-concentrates the draw solution for reuse.

The main problem that restricts the widespread application of the FO desalination process is the establishment of a viable DS and DS recovery system that is potentially capable of continuously and constantly generating high osmotic pressure required for maintaining the water flux at desired levels in the FO process, and at the same time to produce high-quality water with a total elimination of the DS residue in the final product water [5]. Thus, the development of effective DS along with effective DS recovery system with energy-saving remains a significant challenge for FO seawater desalination applications [6–8].

An ideal FO draw solution should meet three main requirements, namely, high osmotic pressure for high water flux, simplistic regeneration method with low-energy consumption, and minimum reverse solute flux for low replenishment cost [9,10]. Most of the research studies are limited to laboratory level studies by using conventional inorganic solutes and polyelectrolyte DS [11]. The conventional inorganic DS can generate high water flux, but the corresponding reserve flux of solute is also high [12,13]. Polyelectrolytes with relatively high molecular weight have been investigated as FO draw solutes and observed that it can reduce reverse flux and can be regenerated using ultrafiltration and membrane distillation [14]. The polyelectrolyte DS based on the thermoresponsive property has also attracted increasing attention due to their high affinity to extract water from seawater, temperature sensitivity and easy regeneration by phase separation technique at elevated temperature [15–17].

The thermoresponsive draw solutes possess lower critical solution temperature (LCST) at which they are miscible with water and show potential to extract water from lower osmotic feed solution partitioned by a semipermeable membrane. The extracted water could be easily separated from the miscible phase by heating the solution to its phase separation temperature. Since the phase transition temperature of LCST materials can be controlled by altering the chemical structure, the energy requirement for the separation of draw solutes can be greatly reduced by using an LCST material with a low phase transition temperature [18]. Thermally responsive draw solutes are attracting researchers due to its simplicity, the absence of using extra chemicals and, most of all, the possibility of using less expensive and clean energy sources such as solar thermal energy and low-grade industrial waste heat for their recycling [19]. TSI has developed a hybrid FO- thermal separation (FO-TS) pilot-scale system using the thermoresponsive polymer for seawater desalination. The FO-TS technology is potentially capable of consuming 87.5% less energy than the conventional RO by using solar energy or waste heat [20].

FO-TS technology is insensitive to the osmotic pressure since it can be operated with higher DS concentrations than that of the FO-RO process. However, there is a potential of having trace amounts of polymer in the final product water. Therefore, a post-treatment system using conventional membrane processes, such as NF or brackish water (BW) RO membrane, may still be needed to polish the product water to meet the WHO standards. Cai and Hu stated that pilot scale studies on thermally responsive organic compounds are substantially needed as there is no information and data on the viability and efficiency of the FO technology for seawater desalination [21]. Shibuya et al. performed an experimental and theoretical study to evaluate the performance of a large-scale hollow fiber (HF) FO module [22]. This study investigated the operating conditions, such as the inlet flow rate, membrane orientation, salt concentration, and salt type, on the module performance of a 5-inch-scale HF module with a cross-wound HF configuration. The theoretical data provided beneficial knowledge not only for predicting module performance but also HF module design parameters, such as recovery ratio, operation conditions, and energy consumption, for full-scale FO processes. A study by Kim et al. analysed the structural features of a spiral-wound forward-osmosis (SW FO) membrane module via an experimental approach and presented the relationships between the water flux and operating conditions for design and operation of a large-scale FO process [23]. This study provided the data on the dependence of pressure drop on flow to determine the optimal flow rate and pressure drop in a commercial SW FO module. In addition, the relationships between water permeate flow and operating conditions (such as flowrate, solution temperature, and osmotic pressure) for the design and operation of a large-scale FO process was demonstrated. Both the previous studies used NaCl as DS, to the best of our knowledge, no simulation study is reported in the literature using the combinations of commercial-scale FO membrane and thermo-responsive polyelectrolyte DS at pilot scale level for the real seawater desalination.

In the literature poly(*N*-isopropylacrylamide) with LCST = 32 °C [24], di(ethylene glycol)*n*-hexyl ether with LCST = 20 °C [25], di(propylene glycol)*n*-propyl ether with LCST = 20 °C [22], propylene glycol *n*-butyl ether with LCST = at all temperature in between 0 and 100 °C [25], poly(*N*-isopropylacrylamide-*co*-acrylic acid) with LCST = 70 °C [26] and copolymer of *N*-isopropylacrylamide (NIPAM) and 2-acrylamido-2-methylpropanesulfonicacid with LCST = 55 °C [27] have been explored as thermo-responsive polyelectrolyte DS for FO process. However, in the current study a polyelectrolyte DS with an acceptable osmotic pressure for the specific seawater desalination application with a cloud point temperature of around 85 °C is used [20]. The solubility of the draw solute decreases significantly with temperature however, it has enough solubility at ambient conditions to provide a useful working osmotic pressure. The draw solute copolymer consists of diol functional groups which impart the required solution properties. The properties of the draw solute such as osmotic pressure, cloud point temperature, and molecular weight desired for the FO application are adjusted by the controlled polymerization reaction. As presented in Table 1, the DS has high osmotic pressure above the concentration of 40% to produce high recovery using seawater feed. The DS was typically selected for the specific seawater desalination application with a strong solubility in water at the lower temperature range (e.g., closer to 40 °C) to minimize the operating temperature of the regeneration steps in the process and to minimize resulting energy loss. The chemistry (molecular weight) and the physical properties of the DS of (osmotic pressure and cloud point temperature) were tailored to attain high rejection in the subsequent post treatment process using NF filtration. Further, the draw solute polymers are selected to minimize back diffusion of the solute through a forward osmosis membrane.

This study will provide the initial findings of FO pilot scale seawater desalination of 10 m^3/day capacity using commercial hollow fiber FO membrane and thermoresponsive polymer DS. This study covers the feasibility of using a thermoresponsive polyelectrolyte DS in a pilot

Table 1
The osmotic pressures and viscosity of DS at different concentrations.

DS concentration (%)	Osmotic pressure (atm)	Viscosity (cP)	
	at 25 °C	at 25 °C	at 85 °C
30	40	49.85	12.85
40	45	69. 07	16.94
50	60	86.90	21.74
70	95	194.48	23.714

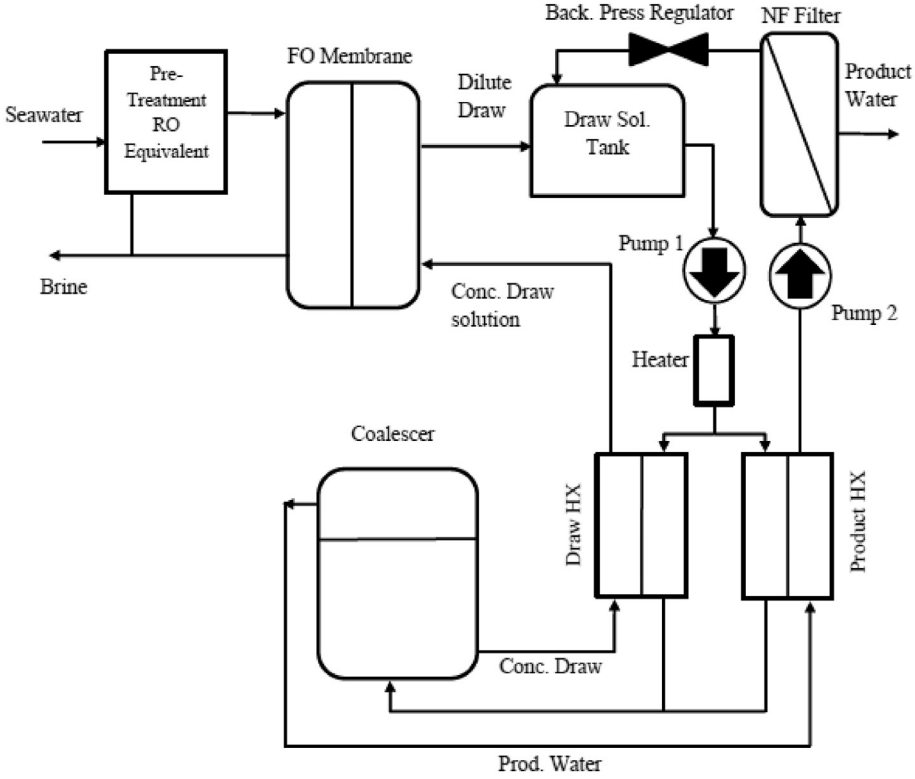

Fig. 1. Schematic diagram of the pilot-scale test unit.

scale FO system, effect of DS flow rates on the distribution of water recoveries over the membrane module, and scope for the improvements over the DS physical properties for the improved performance.

2. Materials and methods

2.1. Materials

The FO pilot plant test unit with a capacity of 10 m^3/d was procured from Trevi Systems Inc., USA. The Trevi Systems' FO pilot plant is designed for continuous operation. The FO pilot plant is a hybrid unit of four processes; pre-treatment system and antiscalant dosing; FO process; polymer draw solution regeneration process; and the post-treatment system. The pre-treatment side consisted of the feed pump, cartridge filters, anti-scalant dosing, pH sensors, temperature sensors and conductivity recorders (Fig. 1). The FO part consisted of DS pump, various valves and sensors and the FO membrane module. The DS regeneration part consisted of three heat exchangers, stainless steel coalescer, heater loop, and various sensors and automated valves. The post-treatment system comprises of the supernatant pump, nano-filters, product water polishing tanks, and assorted automated valves and sensors.

The membrane used was recently developed commercial 10-inch HF FO membrane from Toyobo, Japan. The HF membrane is made of cellulose triacetate and has a bore diameter of 230 μm, inner diameter 230 μm, outer diameter 375 μm, number of fibers: 230,671, and effective membrane area of 336 m^2. The HF FO membrane was specially designed for FO application with cross-wound structures with high packing density and preferable flow pattern compared with another module configuration [22]. The schematic illustration of the tested HF FO module with cross-wound configuration is shown in Fig. 2. The packing density was approximately 55% around a central core tube from which the polymer DS was supplied.

The polymer draw solution used was ethylene oxide-propylene oxide copolymer (TL-1150-1) developed by Trevi systems Inc. having phase separation temperature of 85 °C. The general chemical structure of ethylene oxide-propylene oxide copolymer draw solute is presented in Fig. 3. The copolymer with a molecular weight of approximately 2000 Da was used. The phase separation temperature of the DS recovery system was maintained in a coalescer system connected to heat exchangers. The osmotic pressure and viscosity of polymer DS at various concentrations is shown in Table 1. The system was connected to the nanofiltration post-treatment system to recover any traces of polyelectrolyte solute from the product water. The NF system consisted of NF270-4040 membrane from Filmtec™ membranes with molecular weight cutoff in the range of 200–400 Da. The feed solution used was seawater obtained from the beach well of Doha Research Plant, located near the Doha east power generation and water desalination plant of Kuwait. The physicochemical analysis of the seawater is presented in Table 6 and it has a steady temperature of around 25 °C.

2.2. Methods

The beach well seawater is passed to the bore side of the FO membrane at pressure ~2 bar. The direction of the feed flow was in the axial direction. The DS which is heated to 85 °C is passed to the DS heat exchanger and cooled to temperatures lower than 40 °C. The DS is then passed to the shell side of the FO membrane through the centre core. The direction of the DS flow was in the radial direction between HF tubes. As the FS and concentrated DS flows through the bore side and shell side of the semi-permeable membrane respectively. The DS is infused with and diluted by the pure water that has left the FS. The diluted DS is then fed to the DS recovery systems consisting of coalescer and heat exchangers which are set at temperatures higher than the phase separation temperature of the DS. As a result, the diluted DS is separated into supernatant water and concentrated DS. The concentrated DS is again circulated back to the FO membrane system for further water production and the process continues. The supernatant water is then passed through the post-treatment NF system and heat exchangers and final product water are produced. The flow rates,

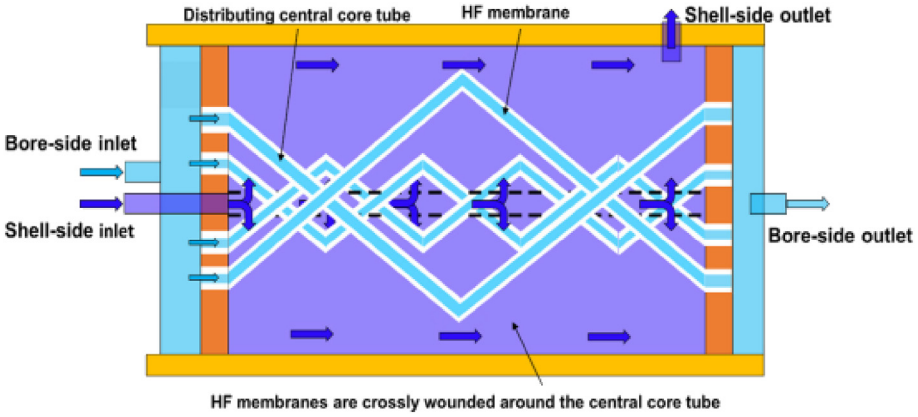

Fig. 2. Schematic of FO HF module with a cross-wound HF configuration.

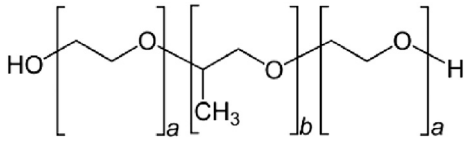

Fig. 3. The general structure of ethylene oxide-propylene oxide copolymer draw solute.

conductivity, pressure, and temperature of all streams were recorded using a data logging system.

2.3. Osmotic pressure measurement

The osmotic pressures of the concentrated and diluted DS were measured using a Wescor 5600 vapor pressure osmometer. The osmolality (m, mol/kg) of DS was measured for DS and then, the osmotic pressure was theoretically calculated using the following Eq. (1) [28,29].

$$\pi = \mathrm{m}\,\rho RT \tag{1}$$

where π is the osmotic pressure, ρ is the density of water, and R and T are the ideal gas constant and absolute temperature, respectively. The theoretically calculated value is then compared with the osmotic pressure value obtained from the refractive index measurements using Atago PAL-RI meter.

2.4. Calculation of DS concentration distribution in HF module

For simulation studies, the HF FO module is divided into 10 blocks into axial and radial directions. The simulation software was developed and supplied by Toyobo Co, Japan. The DS concentration at any block is calculated based on the values of the flow rate, concentration, and pressure of DS and FS of its neighbouring blocks. Fig. 4 presents the division of FO membrane module into different blocks along the axial direction (j = 1 − n), and radial direction (i = 1 − m, where m = 10), where m = n = 10 in the current simulation study. The volume of permeation through each small block (i, j) is denoted as $V_{(i,j)}$, while the volume of salt passing through each block (i, j) is denoted as ws_{ij}. The FS entering into the block (i, j) through the axial direction and its flow rate is denoted as $Q_{FS(i,j-1)}$, concentration as $C_{FS(i,j-1)}$, and pressure as $P_{FS(i,j-1)}$. The DS entering into the block (i, j) through the radial direction and its flow rate is denoted as $Q_{DS(i-1,j)}$, concentration as $C_{FS(i-1,j)}$, and pressure as $P_{FS(i-1,j)}$. The concentration of DS ($C_{DS(i,j)}$) at a block (i, j) is calculated by the Eq. (2). The $C_{DS(i,j)}$ calculations include the boundary conditions of $Q_{DS(in)} = Q_{DS(out)}$, (i.e., permeate flow of DS entering into block (i, j) = permeate flow of DS out from block (i, j)), $C_{DS(in)} = C_{DS(out)}$, (i.e., concentration of DS entering into block (i, j) = concentration of DS out from block (i, j)), $P_{DS(in)} = P_{DS(out)}$, (i.e., the pressure with which DS entering into block (i, j)) and the pressure with which DS out from block (i, j), and $P_{FS(out)} = 0$ (i.e., pressure of FS moving out from block (i, j) = 0).

$$C_{DS(i,j)} = \frac{Q_{DS(i-1,j)} \bullet C_{DS(i-1,j)} - ws_{ij}}{Q_{DS(i,j)}} \tag{2}$$

Similarly, the concentration of FS in the block (i, j) is calculated by applying the above-mentioned boundary conditions using the Eq. (3).

$$C_{FS(i,j)} = \frac{Q_{FS(i,j-1)} \bullet C_{FS(i,j-1)} + ws_{ij}}{Q_{FS(i,j)}} \tag{3}$$

where $C_{DS(i-1,j)}$ is the concentration of FS in the block (i − 1, j).

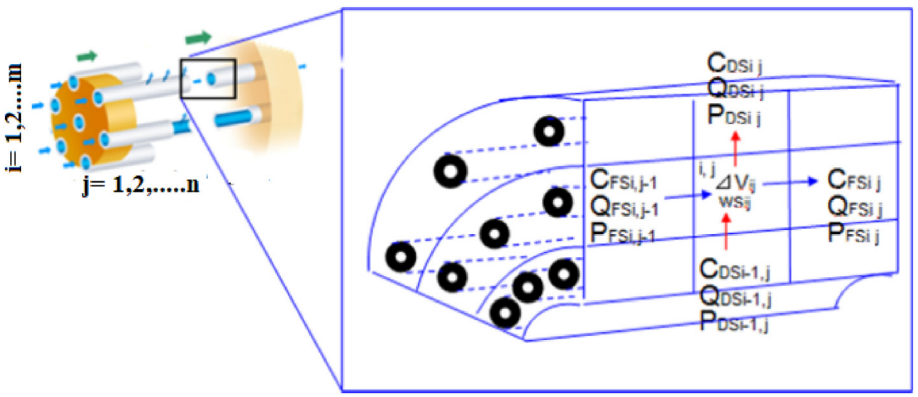

Fig. 4. The schematic presentation of the DS concentration distribution influenced by flow rate, concentration and pressure of DS and FS of its neighbouring blocks.

2.5. Water quality analysis

The pH and conductivity were measured by SI analytics instrumentation, Total Dissolved Solids (TDS) were measured by Thermo Scientific instrument. The other parameters such as calcium, magnesium, chloride, and sulfate were estimated by Ion Chromatography System (ICS), whereas, boron and sodium are estimated by Inductively Coupled Plasma Optical Emission Spectrometry (ICP-OES). The parameters such as nitrate, copper, chromium, iron, silica, phosphate, and fluoride are estimated by spectrophotometer (DR-6000). All analysis was done in triplicate and average values were taken for analysis.

3. Results and discussions

3.1. Influence of DS flow rate on system performance

The DS flow rate was varied from 8 to 18 L/min while keeping the FS flow rate constant. The DS is distributed to the shell side of the membrane through a central core tube in the membrane module as shown in Fig. 2. The DS then flows radially through the membrane module and the concentration of the DS will be the highest at the area near to the centre tube. As it flows radially through the membrane between the HF tubes it gets diluted due to permeation of water molecules from the feed and will be of less concentration as it reaches the area far to the centre tube. So, with increasing flow rate of DS, it is possible to have less DS concentration gradient radially across the membrane. The simulation values of DS concentration in the innermost and outermost layers of the FO module are shown in Table 2. The lower concentration gradient across the membrane at higher DS flow rates resulted in overall high-water flux and product flow rate as shown in Table 3.

In addition, the higher DS flow rate might reduce the thickness of the polymer layer on the membrane surface and thus reduces the concentration polarization effect [30,31]. It was observed that the effect of DS flow rates on product water flow rate and water recovery is not linear and this could be due to the limited capacity of the heat exchangers and, limited separation capacity of coalescer used in the current system. As the DS flow increases the residual time of the polymer in the coalescer was reduced, which reduced enough phase separation time between polymer DS and supernatant water. As presented in Table 4, as the inflow rate of DS increases from 8.1 and 18.1 lpm, the DS concentration at the innermost layer of the membrane dropped from 76.6 to 66.0%. Further increase in DS flowrate decreases the FS concentration gradient in the HF membrane module. The simulated FS concentration in the axial direction of the innermost HF tubes is shown in Table 5. From literature, an increased flow rate across the FO membrane will enhance the water flux due to reduced concentration polarization (CP) effect and the enhanced mass transfer coefficient [30,32]. Thus, the increased flow rate of DS increased its distribution more towards the membrane boundary layer by reducing the thickness of the CP layer.

Table 2
DS concentration distribution in the HF FO module.

FS flow rate (lpm)	DS flow rate (lpm)	inner layer DS concentration (%)	outer layer DS concentration (%)
16.0	8.1	76.6	38.0
	10.1	76.1	40.7
	12.1	76.0	42.7
	14.1	73.7	46.3
	16.1	64.6	43.7
	18.1	66.0	48.8

Table 3
Effect of DS flow rate on production capacity and water recovery ratio.

FS flow rate (lpm)	DS flow rate (lpm)	capacity (m^3/d)	recovery ratio (%)
16.0	8.1	5.5	23.7
	10.1	6.3	28.8
	12.1	7.0	31.2
	14.1	7.2	31.1
	16.1	7.1	29.9
	18.1	6.5	28.9

3.2. Influence of FS flow rate on system performance

The pilot plant was tested at two FS flow rates, 14 and 16 lpm. Table 5 revealed that higher FS flow rates are recommended to increase the product flow rate. The FS is distributed to the bore side of the membrane and it flows in the axial direction as shown in Fig. 4. As the FS flows from the inlet to the outlet side, the polymer DS extracts water and the FS will get concentrated as it reaches the outlet. The DS will be at a high concentration near the central core tube. Thus, at the FS outlet, the FS in the HF tubes near the central core tube will be highly concentrated. Therefore, as the flow rate of FS increases the rate of dilution of the FS near the centre tube will increase. This will again increase the osmotic pressure difference between the DS and FS as a driving force of the process and apparently, both the product water capacity and recovery ratios increased. From Table 5, the product flow rate and water recovery were influenced by flow rates of both the FS and DS. For any increase in the flow rate of DS there was a negligible hydraulic pressure gradient ($\Delta P \sim 0$) across the membrane, since the DS coalescer tank was connected to DS re-circulation and NF post treatment systems. However, an increase in hydraulic pressure gradient across the membrane was observed for the increase in FS flow rate and its ΔP values are presented in the revised Table 5. A combination of FS flow rate, 14 lpm and DS flow rate, 14.1 lpm correspond to an optimum water recovery of 31.3%. In FO, the maximum feed flow is related to the pressure drop across the membrane module [33]. Therefore, above mentioned flow rates of FS and DS could be corresponding to the high osmotic pressure difference across the membrane as driving force of the process favouring the high product flow rate. There is an also increased effect of external concentration polarization due to the lower thickness of the membrane support layer which limit the further increase in flow rate across the FO membrane.

3.3. Influence of DS concentration distribution on system performance

The concentration of polymer DS was not uniform in the HF FO module. The distribution of DS concentration for a run with FS and DS flow rates 16 and 12 lpm respectively is shown in Fig. 5.

The DS concentration is about 76% in the block near to the central core tube and it gradually decreased to 44% as it reaches the outermost layer. This shows that osmotic pressure of DS decreases in the radial direction and hence the water recovery distribution. The HF tubes near the central core tube will have more water recovery percentage than those far from the central core tube.

Similarly, for the same test run, the FS concentration distribution is shown in Fig. 6. The FS concentration at the inlet and outlet of the innermost HF tube near to the central core tube is 35,316 and 113,159 respectively, whereas, the FS concentration at the inlet and outlet of the outermost HF tube far from the central core tube is 35,316 and 40,833 respectively. These data clearly validate the fact that water recovery distribution inside the membrane is not uniform and will be the highest in the innermost HF tubes which are nearest to the concentrated DS with high osmotic pressure.

As the DS flow was increased to 16 lpm the DS concentration in the outermost layer increased to 46% from 44% with 12 lpm DS flow rate. Further increase in DS flowrate to 18 lpm resulted in boundary layer DS

Table 4
FS concentration distribution in the innermost HF tubes at different DS flow rates.

FS flow rate, lpm	DS flow rate, lpm	Innermost layer feed concentration in axial direction										
		1	2	3	4	5	6	7	8	9	10	11
16.0	8.1	35,209	40,667	47,842	57,553	71,097	90,438	117,922	153,489	187,203	203,298	206,002
	10.1	35,270	38,796	43,002	48,080	54,286	61,963	71,560	83,629	98,754	117,277	138,665
	12.1	35,316	38,397	41,991	46,222	51,249	57,276	64,565	73,441	84,279	97,450	113,159
	14.1	35,331	37,675	40,306	43,274	46,639	50,470	54,853	59,886	65,683	72,368	80,067
	16.1	34,429	36,565	38,926	41,544	44,453	47,687	51,286	55,286	59,722	64,620	69,989
	18.1	33,044	34,573	36,226	38,014	39,953	42,058	44,347	46,837	49,548	52,501	55,716

Table 5
Effect of FS flow rate on product water flow rate and water recovery.

DS flow Rate, (lpm)	product capacity (m^3/d)		recovery ratio (%)			
	FS flow rate 14 (lpm)	FS flow rate 16 (lpm)	FS flow rate 14 (lpm)	ΔP[a] (psi)	FS flow rate 16 (lpm)	ΔP (psi)
8.1	5.3	5.5	26.1	4.0–5.0	23.7	6.0–6.5
10.1	6.0	6.3	30.2	4.0–5.0	28.8	6.0–6.5
12.1	6.2	7.0	31.2	4.0–5.0	30.1	6.0–6.5
14.1	6.4	7.2	31.3	4.0–5.0	31.1	6.0–6.5
16.1	5.7	7.1	27.9	4.0–5.0	29.9	6.0–6.5
18.1	5.4	6.5	28.1	4.0–5.0	28.9	6.0–6.5

[a] ΔP; hydraulic pressure gradient across the membrane.

concentration of 50%. This indicates that with the increase in DS flowrate, the DS distribution towards the membrane boundary layer also increases. In FO process, the high difference in osmotic pressure across the membrane and correspondingly high-water fluxes are generally considered to cause severe concentration polarization effects [34]. As a result, the DS concentration gradient across the membrane reduced with a drop-in water recovery gradient in the innermost layer of the membrane, however, overall water recovery of the system increased.

3.4. FO pilot plant product water quality

The FO pilot system has demonstrated a great potential to reduce seawater TDS to 143 ppm in a single stage FO pass over a period of 30 days operation (Table 6). The rejection of boron by the HF FO membrane is highly noticeable as it was reduced from 2.75 to 0.24 mg/L, which is practically not achievable from a single stage RO. The leaking of the polyelectrolyte solute into the final product water was tested by measuring the refractive index values. The results indicated no traces of the polyelectrolyte solute and demonstrated the suitability of NF as a post-treatment process for the product water treatment.

3.5. Scope for improving the DS

The current FO pilot scale system utilized a thermoresponsive DS having property to separate from the diluted water through thermal treatment. The DS concentration during the FO operation has fluctuated in the range of 60–70% (correspond to diluted DS) and 80% (correspond to the initial DS concentration). The curves provided in Fig. 7 are based on the experimental study and are specific regarding the thermoresponsive polyelectrolyte DS selected in this study. As presented in Fig. 7 (blue curve), the phase separation temperatures were measured by heating the different concentrations of polyelectrolyte DS. For any concentration, the DS has shown > 60 °C of phase separation temperature, however, the actual phase separation temperature applied in the DS regeneration system was 85 °C for the effective separation of supernatant water and concentrated DS. This is mainly due to the

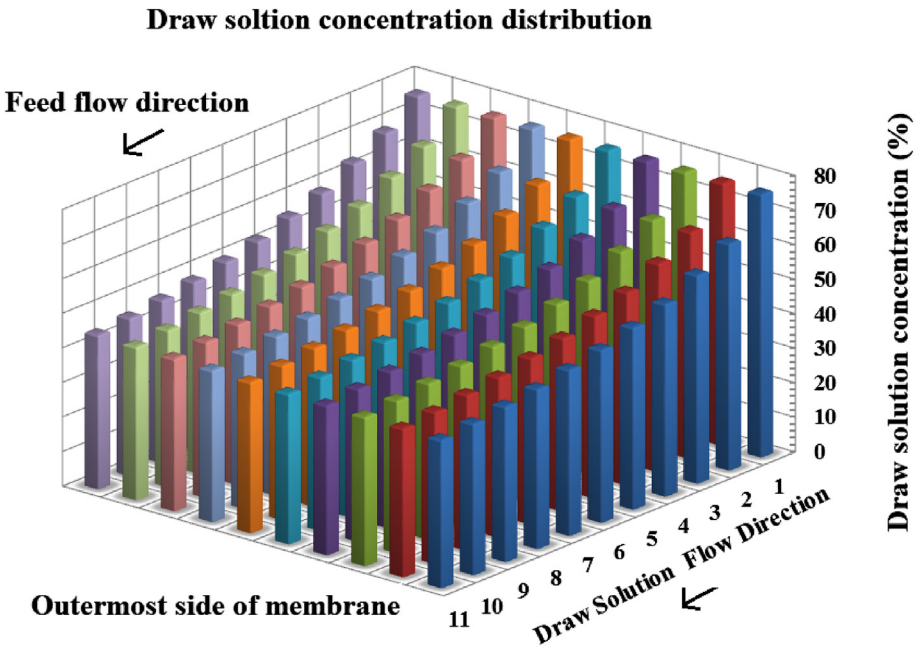

Fig. 5. DS concentration distribution in HF FO membrane (test conditions: flow rates of FS and DS are 16 and 12 lpm respectively).

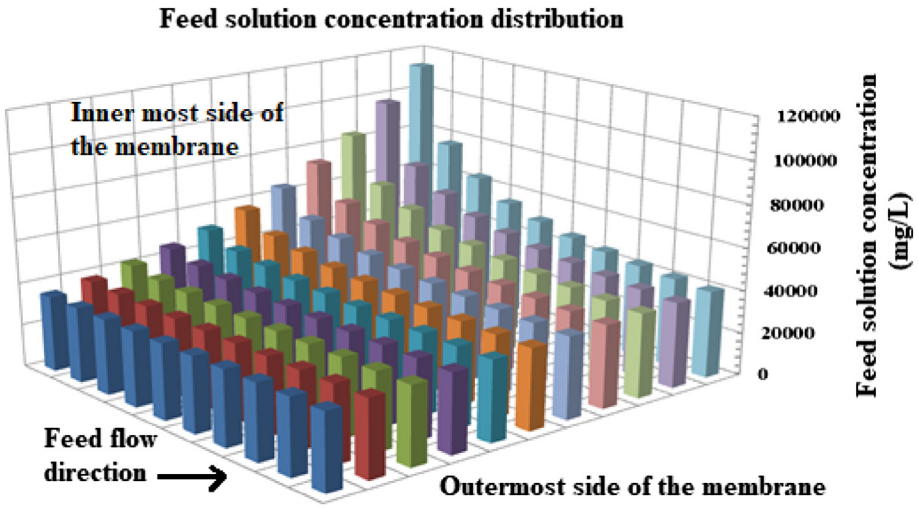

Fig. 6. FS concentration distribution in HF FO membrane.

Table 6
Physiochemical analysis of seawater feed, and FO product.

Parameter	Unit	Seawater Feed	FO Product
pH		7.4	7.2
Conductivity	mS/cm	55.4	0.29
TDS	ppm	35,801	143
Calcium	mg/L	824	6.16
Magnesium	mg/L	1154	5.83
Sulfate	mg/L	3600	0
Chloride	mg/L	26,000	38
Sodium	mg/L	14,800	65
Boron	mg/L	2.75	0.24
Nitrate	mg/L	3.5	0.7
Copper	mg/L	< 0.05	< 0.05
Chromium	mg/L	< 0.05	< 0.05
Iron	mg/L	< 0.05	< 0.05
Silica	mg/L	16.2	0.724
Phosphate	mg/L	0.15	0.11
Fluoride	mg/L	4.3	0.13

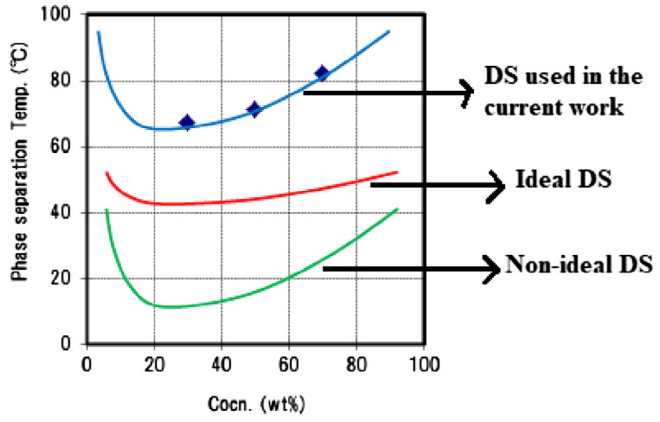

Fig. 7. The Influence of DS concentration on phase separation temperatures indicating ideal and non-ideal DS for future work.

increase in phase separation temperature of the polyelectrolyte DS with the increase in concentration from 30 to 70% (see Fig. 7). Therefore, based on the experimental study a red curve is proposed in Fig. 7 representing the ideal conditions for DS. The ideal conditions represent the phase separation temperature of > 40 °C for any concentrations of the DS to reduce the operating temperature of the DS regeneration system and to avoid any polymer precipitation within the membrane module. The lower phase separation temperature is better; however, it should not be too low to occur the phase separation in the membrane element itself. Such a condition is represented as a non-ideal DS in Fig. 7 (green curve).

The DS for the selected membrane and coalescer tank capacity have witnessed an optimum performance at a phase separation temperature of 85 °C. The phase separation temperature was maintained well above the actual phase separation temperature (i.e. ~80 °C corresponding to 60–70% dilution) to avoid chances of concentration gradient that could take place near the membrane surface during mixing process in the coalescer (Fig. 8). Fig. 7 reveals the phase separation temperature of the DS used in the current study which is well above 60 °C. However, this study recommends a further scope for the improvement of the DS and conditions of the ideal DS as indicated in Fig. 7. This study revealed that the DS with the phase separation temperature of > 40 °C corresponding to any of its concentration will further reduce the temperature required for the process. The lower phase separation temperature is better; however, it should not be too low to occur the phase separation in the membrane element itself. Such a condition is represented as a non-ideal DS in Fig. 7.

3.6. FO pilot plant energy requirement

Among the commercially established desalination technologies, the energy consumption of a thermal based MSF plant is around 70–78 kWh/m^3 [35,36]. The electrical energy equivalent based on power plant efficiency of 30% is around 23.5 kW h/m^3 [35]. The electricity consumption of the pumps ranges between 2.5 and 5.0 kW h/m^3; therefore, the total equivalent energy consumption of the MSF unit is around 27.25 kWh/m^3 [35]. The multiple-effect distillation (MED) process also requires two types of energy-low temperature heat for evaporation and electricity for pumps. The thermal energy consumption of MED plant is around 62.0 kWh/m^3 [35]. The electrical energy equivalent to this value based on a power-plant efficiency of 30% is around 19.1 kW h/m^3 [35]. The total electricity consumption of the pumps ranges from 2.0 to 2.5 kW h/m^3 [37]; therefore, the total equivalent energy consumption of the MED unit is around 21.35 kWh/m^3 [35]. The least energy intensive method is RO with nearly 4 to 6 kWh/m^3 at 50% recovery [35,37,38]. The membrane-thermal based membrane distillation (MD) is not commercially available in the market in large scale and the solar integrated MD has energy consumption in the range of 150–200 kWh/m^3 [35].

In this study, two separate power meters were connected to the FO pilot plant, one that measures the power requirement for the FO pilot plant without the heat generator, and the other one for the electrical

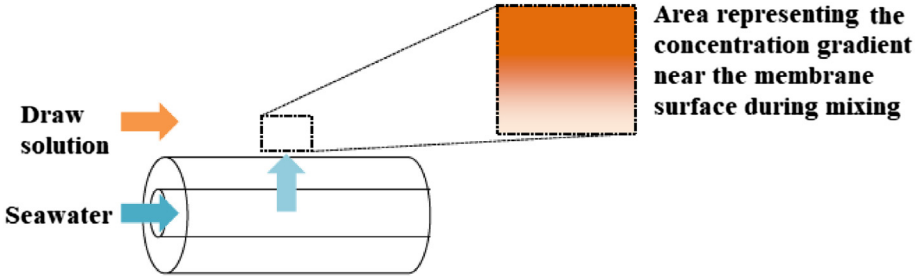

Fig. 8. The schematic presentation of the membrane area facing the concentration gradient at insufficient phase transition temperature.

heater only. The preliminary calculation of energy required by the conventional electrical heater for DS recovery in the FO pilot plant is approximately 35–40 kWh/m^3. It is worthwhile to note that the total energy consumption by the FO pilot plant without the conventional electrical heater of the DS recovery system was around 2.4 kWh/m^3. However, the PLC and control panel used in the pilot plant test unit was consuming around 1.4 kWh/m^3 and this figure was experimentally observed. This value is quite high because of the low production capacity of the tested pilot plant. This value can be drastically reduced by increasing the permeate capacity of the FO pilot plant. In general, the very low energy requirement by the FO pilot plant was due to the absence of high-pressure pumps. The maximum pressure required by the FS pump, DS recirculating pump, and supernatant pump were < 2, 1 and 3 bar, respectively. It was observed > 90% of the total energy consumed is used by the conventional electrical heater of the DS recovery system of the tested pilot plant. The results from the current study show that the tested FO pilot plant can produce freshwater with an energy requirement less than the minimum energy for SWRO, provided the energy needed for DS recovery is supplied in the form of low-grade industrial waste heat or solar thermal energy.

4. Conclusion

This study evaluated the feasibility of using thermoresponsive DS for seawater desalination at pilot scale level. The FO pilot plant over a continuous operation of 30 days was capable to produce product water of TDS ~150 ppm at water recovery ratio of ~30%. The performance of the polyelectrolyte DS mainly relies on the flow rates of the DS and FS applied in the system. The general assumption made from the study is that the high flow rate of DS it is possible to have less DS concentration gradient radially across the membrane resulted in overall high-water flux and product flow rate. The observed high-water flux with increased DS flow rate is also due to reduced concentration polarization. The increased FS flow rate increases the rate of dilution of the FS to increase the osmotic pressure difference between the DS and FS. As a result, both the product water capacity and recovery ratios increased. Though the DS in the current study showed high performance at phase transition temperature of 85 °C, yet there is a scope for further research to hunt for the ideal DS with > 45 °C phase transition temperature corresponding to any of its concentration. The study established the fact that the energy requirement of FO can be less than the minimum energy for SWRO by utilizing low-grade industrial waste heat or solar thermal energy for DS recovery. The values of water quality parameters obtained from the FO pilot plant are promising and proved that FO technology can be considered as an alternative desalination process to conventional desalination technologies. Overall, this study provides beneficial information for the implementation of commercial-scale FO desalination system based on the performance results in terms of recovery ratio, and operating conditions using a commercial scale FO module in combination with thermal DS recovery system.

Acknowledgements

Authors are thankful to the Director General of the Kuwait Institute for Scientific Research (KISR) and Executive Director of Water Research Centre, KISR for their continued support and encouragement towards this research.

References

[1] M. Elimelech, W.A. Phillip, The future of seawater desalination: energy, technology, and the environment, Science 333 (2011) 712–717.
[2] P. Wang, Y. Cui, Q. Ge, T. Tew, T. Chung, Evaluation of hydroacid complex in the forward osmosis–membrane distillation (FO–MD) system for desalination, J. Membr. Sci. 494 (2015) 1–7.
[3] T. Cath, Osmotically and thermally driven membrane processes for enhancement of water recovery in desalination processes, Desalin. Water Treat. 15 (2010) 279–286.
[4] Y. Hartanto, M. Zargar, X. Cui, Y. Shen, B. Jin, S. Dai, Thermoresponsive cationic copolymer microgels as high performance draw agents in forward osmosis desalination, J. Membr. Sci. 518 (2016) 273–281.
[5] B. Coday, P. Xu, E. Beaudry, J. Herron, K. Lampi, N. Hancock, T. Cath, The sweet spot of forward osmosis: treatment of produced water, drilling wastewater, and other complex and difficult liquid streams, Desalination 333 (1) (2014) 23–35.
[6] R.V. Linares, Z. Li, S. Sarp, S. Bucs, G. Amy, J.S. Vrouwenvelder, Forward osmosis niches in seawater desalination and wastewater reuse, Water Res. 66 (2014) 122–139.
[7] K. Lutchmiah, A.R.D. Verliefde, K. Roest, L.C. Rietveld, E.R. Cornelissen, Forward osmosis for application in wastewater treatment: a review, Water Res. 58 (2014) 179–197.
[8] A. Mahto, D. Mondal, V. Polisetti, J. Bhatt, M.R. Nidhi, K. Prasad, S.K. Nataraj, Sustainable water reclamation from different feed streams by forward osmosis process using deep eutectic solvents as reusable draw solution, Ind. Eng. Chem. Res. 56 (49) (2017) 14623–14632.
[9] Q. Ge, J. Su, G.L. Amy, T.S. Chung, Exploration of polyelectrolytes as draw solutes in forward osmosis processes, Water Res. 46 (2012) 1318–1326.
[10] L. Chekli, S. Phuntsho, H.K. Shon, S. Vigneswaran, J. Kandasamy, A. Chanan, A review of draw solutes in forward osmosis process and their use in modern applications, Desalin. Water Treat. 43 (2012) 167–184.
[11] Y. Cai, W. Shen, J. Wei, T.H. Chong, R. Wang, W.B. Krantz, A.G. Fane, X. Hu, Energy-efficient desalination by forward osmosis using responsive ionic liquid draw solutes, Environ. Sci.: Water Res. Technol. 1 (3) (2015) 341–347.
[12] J.S. Yong, W.A. Phillip, M. Elimelech, Reverse permeation of weak electrolyte draw solutes in forward osmosis, Ind. Eng. Chem. Res. 51 (41) (2012) 13463–13472.
[13] A. Achilli, T.Y. Cath, A.E. Childress, Selection of inorganic-based draw solutions for forward osmosis applications, J. Membr. Sci. 364 (2010) 233–241.
[14] M.M. Ling, T.-S. Chung, Surface-dissociated nanoparticle draw solutions in forward osmosis and the regeneration in an integrated electric field and nanofiltration system, Ind. Eng. Chem. Res. 51 (47) (2012) 15463–15471.
[15] M.M. Ling, T.-S. Chung, X. Lu, Facile synthesis of thermosensitive magnetic nanoparticles as “smart” draw solutes in forward osmosis, Chem. Commun. 47 (2011) 10788–10790.
[16] M. Noh, Y. Mok, S. Lee, H. Kim, S.H. Lee, G.-W. Jin, J.-H. Seo, H. Koo, T.H. Park, Y. Lee, Novel lower critical solution temperature phase transition materials effectively control osmosis by mild temperature changes, Chem. Commun. 48 (2012) 3845–3847.
[17] H. Han, J.Y. Lee, X. Lu, Thermoresponsive nanoparticles + plasmonic nanoparticles photoresponsive heterodimers: facile synthesis and sunlight-induced reversible clustering, Chem. Commun. 49 (2013) 6122–6124.
[18] H. Kim, S. Lee, M. Noh, S.H. Lee, Y. Mok, G. Jin, J.H. Seo, Y. Lee, Circulatory osmotic desalination driven by a mild temperature gradient based on lower critical solution temperature (LCST) phase transition materials, Polymer 52 (2011) 1367.
[19] X. Zhou, D.B. Gingerich, M.S. Mauter, Water treatment capacity of forward-osmosis systems utilizing power-plant waste heat, Ind. Eng. Chem. Res. 54 (2015) 6378–6389.
[20] Carmignani, G.; Sitkiewitz, S.; Webley, J. Recovery of 448 retrograde soluble solute for forward osmosis water treatment. U. S. Patent 20120267308 A1, 2012.
[21] Y. Cai, X. Hu, A critical review on draw solutes development for forward osmosis,

Desalination 391 (2016) 16–29.
[22] M. Shibuya, M. Yasukawa, S. Goda, H. Sakurai, T. Takahashi, M. Higa, H. Matsuyama, Experimental and theoretical study of a forward osmosis hollow fiber membrane module with a cross-wound configuration, J. Membr. Sci. 504 (2016) 10–19.
[23] Y.C. Kim, S.J. Park, Experimental study of a 4040 spiral-wound forward-osmosis membrane module, Environ. Sci. Technol. 45 (2011) 7737–7745.
[24] R. Ou, Y. Wang, H. Wang, T. Xu, Thermo-sensitive polyelectrolytes as draw solutions in forward osmosis process, Desalination 318 (2013) 48–55.
[25] D. Zhao, P. Wang, Q. Zhao, N. Chen, X. Lu, Thermoresponsive copolymer-based draw solution for seawater desalination in a combined process of forward osmosis and membrane distillation, Desalination 348 (2014) 26–32.
[26] Y. Wang, H. Yu, R. Xie, K. Zhao, X. Ju, W. Wang, Z. Liu, L. Chu, An easily recoverable thermo-sensitive polyelectrolyte as draw agent for forward osmosis process, Chin. J. Chem. Eng. 24 (2016) 86–93.
[27] T. Mori, S. Sase, K. Kitamura, Forward osmosis using temperature-responsive slurries as a draw solution, American, J. Environ. Eng. Sci. 4 (2017) 20–29.
[28] N.P. Money, Osmotic pressure of aqueous polyethylene glycols relationship between molecular weight and vapor pressure deficit, Plant Physiol. 91 (1989) 766–769.
[29] J. Cheng, M. Gier, L.U. R-Rodriguez, V. Prasad, J.A.W. Elliott, A. Sputtek, Osmotic virial coefficients of hydroxyethyl starch from aqueous hydroxyethyl starch sodium chloride vapor pressure osmometry, J. Phys. Chem. B 117 (2013) 10231–10240.
[30] S. Chakrabortty, M. Pal, M. Roy, P. Pal, Water treatment in a new flux enhancing, continuous forward osmosis design: transport modelling and economic evaluation towards scale up, Desalination 365 (2015) 329–342.
[31] J.E. Kim, S. Phuntsho, F. Lotfi, H.K. Shon, Investigation of pilot-scale 8040 FO membrane module under different operating conditions for brackish water desalination, Desalin. Water Treat. 53 (2014) 2782–2791.
[32] X. Zhang, J.G. Gai, Single-layer graphene membranes for super-excellent brine separation in forward osmosis, RSC Adv. 5 (2015) 68109–68116.
[33] M. Kostoglou, A.J. Karabelas, On the fluid mechanics of spiral wound membrane modules, Ind. Eng. Chem. Res. 48 (2009) 10025–10036.
[34] J.R. McCutcheon, R.L. McGinnis, M. Elimelech, Desalination by ammonia-carbon dioxide forward osmosis: influence of draw and feed solution concentrations on process performance, J. Membr. Sci. 278 (2006) 114–123.
[35] A.A. Karaghouli, L.L. Kazmerski, Energy consumption and water production cost of conventional and renewable-energy-powered desalination processes, Renew. Sust. Energ. Rev. 24 (2013) 343–356.
[36] F. Banat, Economic and Technical Assessment of Desalination Technologies, in: Proceedings of the Seminar on Energy Systems Analysis, 6–8 June 2007, Geneva, Switzerland.
[37] R. Semiat, Energy issues in desalination processes, Environ. Sci. Technol. 42 (22) (2008) 8193–8201.
[38] D. Zarzo, D. Prats, Desalination and energy consumption. What can we expect in the near future? Desalination 427 (2018) 1–9.